PET-RAFT Increases Uniformity in Polymer Networks

Shiwanka V. Wanasinghe^a, Mingkang Sun^b, Kevin Yehl^a, Julia Cuthbert,^b Krzysztof Matyjaszewski^{b*}, Dominik Konkolewicz^{a*}

Abstract

Photoinduced electron/energy transfer (PET)- reversible addition-fragmentation chain transfer polymerization (RAFT) and conventional photoinitiated RAFT were used to synthesize polymer networks. In this study, two different metal catalysts: Ir(ppy)₃ and ZnTPP were selected to generate two different catalytic pathways: with Ir(ppy)₃ proceeding through an energy transfer pathway and with ZnTPP proceeding through an electron transfer pathway. These PET RAFT systems were contrasted against a conventional photoinitated RAFT process. Mechanically robust materials were generated. Using bulk swelling ratios and degradable crosslinkers, the homogeneity of the networks was evaluated. Especially at high primary chain length and crosslink density, the PET-RAFT systems generated more uniform networks than those made by conventional RAFT, with the electron transfer-based ZnTPP giving superior results to those of Ir(ppy)₃. The ability to deactivate radicals either by RAFT exchange or reversible coupling in PET RAFT was proposed as the mechanism that gave better control in PET-RAFT systems.

^a Department of Chemistry and Biochemistry, Miami University, 651 E High St Oxford, OH, 45056, USA

^b Department of Chemistry, Carnegie Mellon University, 4400 Fifth Ave, Pittsburgh, PA, 15213, USA

^{*} Corresponding authors: KM: matyjaszewski@cmu.edu, DK: d.konkolewicz@miamiOH.edu

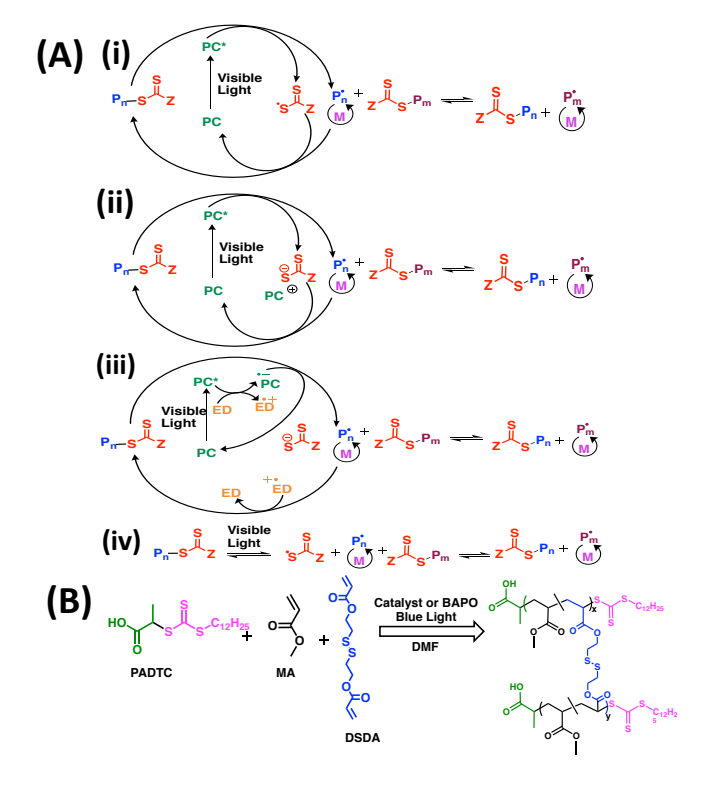
INTRODUCTION

Reversible deactivation radical polymerization (RDRP) methods have been developed over the past decade, allowing controlled polymerization of a wide variety of functional monomers. ^{1,2} In particular, atom transfer radical polymerization (ATRP) and reversible addition-fragmentation chain transfer polymerization (RAFT) have emerged as two of the most commonly used RDRP methods for synthesis of complex polymers including block, gradient copolymers, stars and networks. ³ The improved control over primary chain structure afforded by RAFT and ATRP has led to materials with enhanced properties, including superior adhesives, increased dynamics in polymers and more uniform networks, compared to their analogues synthesized under conventional free radical polymerization (FRP). ⁴ Further, in recent work, although similar network properties could be obtained by both RAFT and ATRP, a direct comparison suggests that ATRP provides better control over the network and its primary chains than RAFT, with both being better controlled than FRP. ⁵ Hence, it is important to explore RAFT methods that can enhance control over the polymer chain, even under challenging network syntheses.

RAFT was first reported in 1998 by Rizzardo and co-workers⁶ and is one of the most versatile RDRP methods. In RAFT, control over the polymer chain occurs through the degenerative transfer between propagating radicals and thiocarbonylthio based chain transfer agents (CTAs). Traditionally, RAFT uses thermal radical initiators to synthesize complex polymers under easily accessible conditions.^{5,7,8} In addition to the traditional RAFT process, several pathways have been developed for activating the RAFT polymerization including: photoinduced electron/energy transfer (PET) RAFT, photoiniferter, electrochemical, enzymatic RAFT.⁹ Photochemically driven RAFT techniques have drawn significant attention over the conventional thermal process due to its mild reaction conditions and the possibility of spatiotemporal control, enabling potential applications such as 3D printed materials.¹⁰ Further, a recent study has reported the differences between photochemical and the traditional thermal RAFT polymerization using block polymers,¹¹ indicating superior livingness for the photochemical approach. In 2022, Foster et al. showed a similar conclusion, demonstrating the superior control of PET-RAFT compared to conventional RAFT using multiblock star polymers.¹²

Initially, photochemically driven RAFT polymerization has been achieved through the UV-based photolysis of CTAs through the photoiniferter process. ^{13–16} However, due to the harsh conditions and potential degradation of the CTA, high energy UV light irradiated systems can be

challenging to implement.¹⁶ More recently, visible light induced RAFT techniques were introduced.^{17–20} PET-RAFT is a visible light triggered RAFT polymerization method which activates CTAs using a photo catalyst.^{9,21} Generally, organic compounds or transition metal catalysts are used as the photocatalyst in PET-RAFT.^{22–24} In PET-RAFT, the CTA acts as both transfer agent and the initiator which react with the photocatalyst to generate radicals. There are three main classes of photocatalyzed mechanisms in PET-RAFT: (i) photoinduced energy transfer, (ii) photoinduced oxidative electron transfer, and (iii) photoinduced reductive electron transfer. The literature suggests that the reaction pathway of a PET-RAFT system depends on the catalyst used for the excitation.²⁵ In addition to these photocatalyzed processes, CTA itself can undergo photoiniferter pathway under visible light via homolytic cleavage to produce radicals, then transfer via RAFT process and terminate reversibly.¹⁶ However, this photoiniferter pathway is minor under typical PET-RAFT conditions.²⁶



Scheme 1: (A) Proposed mechanisms (i) photoinduced energy transfer—RAFT polymerization (E.g. Ir(ppy)₃) (ii) photoinduced oxidative electron transfer—RAFT polymerization (E.g. ZnTPP) (iii) photoinduced reductive electron transfer—RAFT polymerization (iv) photoiniferter polymerization. photocatalyst (PC) electron donors (ED)

(B) Representation of the networks synthesized using photocatalysts or BAPO. PADCT (2-(dodecylthiocarbonothioylthio)propionic Acid)

As noted, previous work indicated that RAFT generates networks that are more uniform, with better controlled chains than FRP, but lower control than ATRP, especially at higher chain lengths.⁵ This was attributed to the high viscosity in a polymer network potentially inhibiting the chain diffusion needed for efficient RAFT exchange. In contrast, ATRP uses small molecule catalysts, which can diffuse more readily in a viscous medium. However, due to the reversible deactivation pathways, PET-RAFT involving both RAFT exchange and reversible coupling with the CTA fragment, PET-RAFT has potential to offer superior control compared to conventional RAFT in network synthesis. This is because the reversible coupling pathway involves a small molecule CTA fragment and the radical, which should be less affected by viscosity than two macromolecular species. This study compares the networks synthesized using PET-RAFT via two different catalytic systems: tris[2-phenylpyridinato-C2,N]iridium(III) (Ir(ppy)₃) and zinc tetraphenylporphyrin (ZnTPP). PET-RAFT using Ir(ppy)₃ has been identified as proceeding through an energy transfer mechanisms, ²⁷ while ZnTPP systems occur through an oxidative electron transfer process.²⁸ In addition to two PET-RAFT systems, conventional RAFT photopolymerization is performed using a traditional photoinitiator, phenylbis(2,4,6trimethylbenzoyl) phosphine oxide (BAPO), using similar conditions compared to the networks prepared by PET-RAFT. This study directly compares the primary chain and network properties of the three photochemical RAFT methods, PET-RAFT using ZnTPP, PET-RAFT using Ir(ppy)₃ and conventional RAFT photoinitiated by BAPO. This study finds that PET-RAFT using ZnTPP leads to superior control over primary chain and network properties.

All the networks were prepared using methyl acrylate (MA) as the monomer; 2,2'dithiodiethanol crosslinker; diacrylate (DSDA) the and 2as (dodecylthiocarbonothioylthio)propionic acid (PADTC) as the CTA under blue light irradiation (Scheme 1B). DSDA was incorporated to evaluate the molecular characteristics of the networks using size exclusion chromatography (SEC) after cleaving the disulfide linkers. The absorbance spectra of BAPO, ZnTPP, Ir(ppy)₃ and PADTC are given in **Figure S1**, with the LED emission spectrum given in Figure S2. In all experiments, a blue light photoreactor was used with an emission peak at 450±10 nm, and an intensity of 35±1 mW/cm². Altogether, 9 samples (Ir(ppy)₃, ZnTPP and BAPO) were prepared by changing the chain length and the crosslink density with compositions given in Table S2. Table 1 represents the molecular characterization and network degradation results. ¹H NMR was used to calculate the total conversion of the monomer and the

crosslinker. The conversion is an important parameter in network characterization since it directly affects the network formation and material properties. Ir(ppy)₃ and BAPO systems demonstrated over 95% conversion for all samples. However, ZnTPP networks reached slightly lower conversions in DP 500 systems. As noted earlier, ZnTPP systems undergo oxidative electron transfer in PET-RAFT. This mechanistic difference could affect the rate of the polymerization of the ZnTPP DP 500 system resulting in lower conversion. Previously, it was reported that the lower rates can be expected for electron transfer systems due to higher energy gaps between excited state and the charge transfer state.²⁸ Moreover, kinetic studies demonstrated that ZnTPP system has longer incubation period of 200/5/1 system (**Figure S3**).

Table 1: Structural characteristics of networks prepared using Ir(ppy)₃, ZnTPP and BAPO. All molecular weights and dispersities determined by Size Exclusion Chromatography after cleavage of disulfide bonds using DTT.

| Catalyst/ BAPO | [MA]/[DSDA]/ [PADTC]* | Conversion (%) | Gel fraction | $\mathbf{M_n}$ | ** |
|----------------------|----------------------------------|--------------------------|--|---|--|
| Ir(ppy) ₃ | 200/5/1 500/5/1 500/12.5/1 | >95 >95 >95 >95 | $0.992 \pm 0.002 \\ 0.984 \pm 0.002 \\ 0.995 \pm 0.001$ | $2.85\pm0.07 \times 10^4$ $3.9\pm0.3 \times 10^4$ $5.44\pm0.06 \times 10^4$ | 1.35 ± 0.05 1.43 ± 0.05 2.2 ± 0.4 |
| ZnTPP | 200/5/1 500/5/1 500/12.5/1 | >95 85 91 | $\begin{array}{c} 0.988 \pm 0.002 \\ 0.990 \pm 0.002 \\ 0.997 \pm 0.002 \end{array}$ | $2.2\pm0.3 \times 10^4$ $4.33\pm0.3 \times 10^4$ $3.6\pm0.2 \times 10^4$ | $\begin{aligned} 1.24 &\pm 0.03 \\ 1.28 &\pm 0.03 \\ 1.35 &\pm 0.08 \end{aligned}$ |
| ВАРО | 200/5/1 500/5/1 500/12.5/1 | >95 >95 >95 | $\begin{array}{c} 0.978 \pm 0.003 \\ 0.985 \pm 0.002 \\ 0.988 \pm 0.001 \end{array}$ | $2.12\pm0.01 \times 10^4$ $4.2\pm0.1 \times 10^4$ $4.2\pm0.1 \times 10^4$ | 1.4 ± 0.05 1.55 ± 0.01 2.1 ± 0.2 |

^{*}The molar equivalents are MA/DSDA/CTA

In addition to total monomer conversion, the gel fraction of the polymers was evaluated. In sol gel fraction experiment, sol fraction refers to the high molecular weight polymers that are not connected to the main network which were removed by dialysis. The ratio between the weight of the sol and the remaining gel fraction was calculated. The gel fractions for all systems are above 95%.

^{**} M_n and dispersity values are corrected using Mark-Houwink-Sakurada Correction

To evaluate the control over the polymer structure and primary chain homogeneity in each system, crosslinker and chain length, degradation of the disulfide linkers in networks was performed, with subsequent SEC analysis. A small piece of each material was de-crosslinked by converting the disulfide crosslinker into thiols using dithiothreitol (DTT). All samples were fully degraded after 24 hrs and the resulting solutions were analyzed by SEC. SEC showed that the ZnTPP materials have slightly lower D values than Ir(ppy)₃ and BAPO at shorter chain length (([MA]/[DSDA/[PADTC]=200/5/1). However, significantly higher D values was observed for BAPO and Ir(ppy)₃ than ZnTPP at higher chain length with high crosslinking density ([MA]/[DSDA/[PADTC]=500/12.5/1). For example, BAPO showed 2.1 ± 0.2 dispersity and Ir(ppy)₃ showed 2.2 ± 0.5 dispersity for the 500/12.5/1 system, while ZnTPP showed 1.37 ± 0.08 . This suggests that ZnTPP is able to control the polymer network better than BAPO and Ir(ppy)₃, even at relatively long chain lengths and high crosslink density. This excellent controllability of the ZnTPP systems was clearly visualized in SEC traces showing narrow distribution in ZnTPP system (Figure 1). BAPO and Ir(ppy)₃ showed similar SEC traces in all systems except 200/5/1 of Ir(ppy)₃, which showed a small shoulder peak. This could be due to the traces of sol present in the networks. The structural controllability of the system was measured by preparing linear polymer models following compositions in **Table S1**, which showed good control at both chain length 200 500 as indicated in Table S3 and Figure S4. Dispersity values of all [MA]/[DSDA]/[PADTC]=200/5/1 and 500/5/1 networks segments are comparable to the respective linear models. However, 500/12.5/1 networks of BAPO and Ir(ppy)₃ gave significantly higher dispersity compared to its linear models indicated by a D above 2.0.

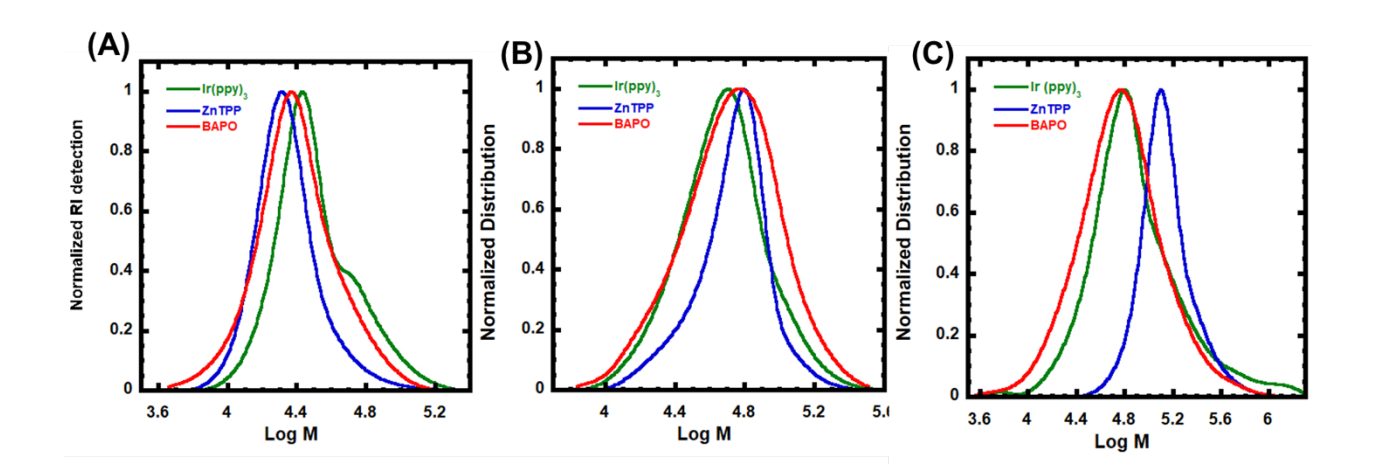


Figure 1: SEC traces of the degraded networks (A) 200/5/1 networks, (B) 500/5/1 networks (C) 500/12.5/1 networks

The network uniformity of a bulk material was investigated by swelling ratio experiments (**Figure 2**). Generally, more homogeneous networks of the same bulk crosslink density are able to absorb more solvent, since they have regular placements of crosslinkers, rather than clusters and domains of high crosslink density which cannot expand efficiently.⁵ ZnTPP showed higher swelling capacities compared to BAPO and Ir(ppy)₃. BAPO and Ir(ppy)₃ had similar swelling ratios in both [MA]/[DSDA]/[PADTC]=200/5/1 of ~3.5-3.6 and 500/12.5/1 of ~3.4-3.5. With the composition [MA]/[DSDA]/[PADTC]=500/5/1 Ir(ppy)₃ had a higher swelling ratio of ~7.1, compared to BAPO which had a swelling ratio of ~6.4. The swelling ratios of the ZnTPP based materials were ~5.0, ~8.3, and ~4.4 at compositions of [MA]/[DSDA]/[PADTC]=200/5/1, [MA]/[DSDA]/[PADTC]=500/5/1, and [MA]/[DSDA]/[PADTC]=500/12.5/1, respectively. The higher swelling ratio in ZnTPP based materials suggests better network uniformity and agrees with the trends in primary chain dispersities. As anticipated the swelling ratio decreased as the crosslink density increased. For systems with similar crosslink densities, but with different chain lengths had similar swelling ratios, albeit slightly lower at the longer chain lengths.

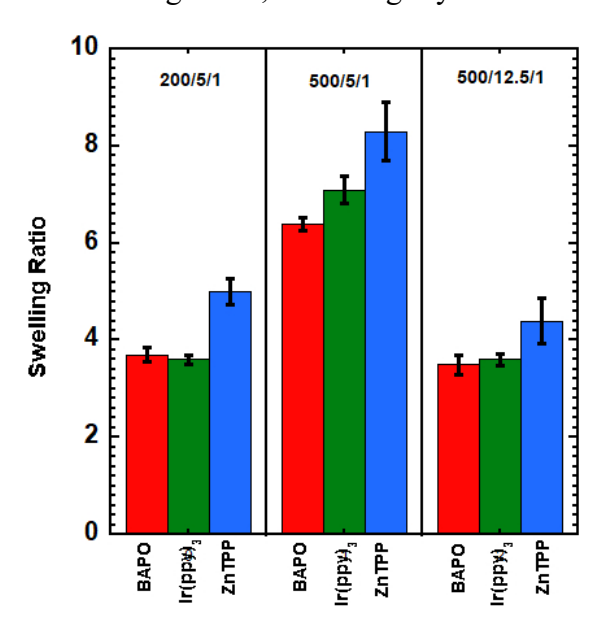


Figure 2: Swelling ratios of networks after soaking in DMF for 48 hrs. Black bars are the standard deviations (n=3)

In addition to measuring the swelling ratios, network properties were evaluated using oscillatory shear rheology in temperature sweep experiments. Minor differences in material properties were observed in the storage moduli or the Tanδ profiles. Glass transition temperatures near 20-30 °C were observed in all cases (**Figure S5**), taken as the peak of the Tanδ curve (**Figure S5**). This suggests that although ZnTPP leads to more uniform chains, with better distribution of crosslinkers in the backbone, this did not translate to a substantial change in the material's mechanical properties.

Overall, the data in this study suggests that PET-RAFT, in particular using ZnTPP as the photocatalyst, can lead to more uniform networks, with superior control over the primary chain length. These differences become most apparent at long chain lengths with a relatively high crosslink density. In these cases, the system should reach the gel point at the lowest conversion, leading to a highly viscous system beyond the gel point. A possible reason for the superior control using ZnTPP is that the proposed electron transfer leads to efficient radical deactivation/exchange through both RAFT degenerative transfer, and back reaction of the radical with the thiocarbonylthiolate group. In contrast, the energy transfer pathway, which dominates Ir(ppy)₃ leads to thiocarbonylthiyl radicals which can potentially eliminate CS₂,²⁹ leading to a decrease in control. The elimination of CS₂ is anticipated to be most significant after the gel point when chain mobility is inhibited and transient radical lifetime is potentially increased. Since the [MA]/[DSDA]/[PADTC]= 500/12.5/1 system should have the lowest gel point, this system is most prone to substantial elimination of CS₂ impacting chain livingness. In the network system, this elimination could be significant, due to poor diffusion between the radical chain end and the thiocarbonylthiyl radical. This is anticipated to lead to a loss of livingness and reduced control. Finally, the control system with BAPO can only have radical deactivation through the RAFT exchange process, which requires diffusion of two macromolecular chain ends (CTA and radical), unlike PET-RAFT that can deactivate radical chain ends though the RAFT exchange but also the intrinsic reversible coupling reactions in PET-RAFT.

CONCLUSIONS

A series of polymer networks of distinct chain lengths and crosslink densities were synthesized by three photochemical RAFT approaches, conventional radical generation from a photoinitiator, BAPO, and PET-RAFT using two photocatalysts, Ir(ppy)₃ and ZnTPP. The PET-

RAFT systems tended to have superior control over primary chain structure, with more uniform

networks. In particular, the ZnTPP catalytic system led to chains with lower dispersity and more

uniform networks capable of reaching a higher swelling ratio. The increase in control over the

primary chain and network properties in ZnTPP based PET-RAFT is due to the PET-RAFT

mechanism allowing two pathways for radical deactivation, the traditional RAFT degenerative

exchange, present in all systems, as well as reversible coupling between the propagating radical

and the CTA/photocatalyst fragments that derive from PET-RAFT activation. The former pathway

could be inhibited in viscous polymer networks, as it relies on diffusion of two macromolecular

chain ends, while the second pathway occurs between a polymeric radical and small molecule,

which are less impacted by diffusional restrictions. These results indicate that PET-RAFT is a

powerful strategy that can lead to superior control over polymer chains, even under challenging

reaction conditions such as network formation.

AUTHOR INFORMATION

Corresponding Authors

Krzysztof Matyjaszewski - Department of Chemistry, Carnegie Mellon University, 4400 Fifth

Ave, Pittsburgh, PA, 15213, USA

Email: matyjaszewski@cmu.edu

Dominik Konkolewicz - Department of Chemistry and Biochemistry, Miami University, 651 E

High St Oxford, OH, 45056, USA

Email: d.konkolewicz@miamiOH.edu

Authors

Shiwanka V. Wanasinghe- Department of Chemistry and Biochemistry, Miami University, 651

E High St Oxford, OH, 45056, USA

Minkang Sun - Department of Chemistry, Carnegie Mellon University, 4400 Fifth Ave,

Pittsburgh, PA, 15213, USA

Kevin Yehl - Department of Chemistry and Biochemistry, Miami University, 651 E High St

Oxford, OH, 45056, USA

ACKNOWLEDGEMENT

The Konkolewicz group gratefully acknowledges support from the National Science Foundation under Grant No. (DMR-1749730) for RAFT materials synthesis and molecular characterization. 400 MHz NMR instrumentation at Miami University is supported through funding from the National Science Foundation under grant number (CHE-1919850). The Matyjaszewski group acknowledges funding from the National Science Foundation (CHE- 2000391) and Department of Energy (grant ER45998) for bulk materials characterization.

REFERENCES

- (1) Parkatzidis, K.; Wang, H. S.; Truong, N. P.; Anastasaki, A. Recent Developments and Future Challenges in Controlled Radical Polymerization: A 2020 Update. *Chem* **2020**, *6* (7), 1575–1588.
- (2) Corrigan, N.; Jung, K.; Moad, G.; Hawker, C. J.; Matyjaszewski, K.; Boyer, C. Reversible-Deactivation Radical Polymerization (Controlled/Living Radical Polymerization): From Discovery to Materials Design and Applications. *Prog. Polym. Sci.* **2020**, *111*, 101311.
- (3) Truong, N. P.; Jones, G. R.; Bradford, K. G. E.; Konkolewicz, D.; Anastasaki, A. A Comparison of RAFT and ATRP Methods for Controlled Radical Polymerization. *Nat. Rev. Chem.* **2021**, *5* (12), 859–869.
- (4) Vakil, J. R.; Watuthanthrige, N. D. A.; Digby, Z. A.; Zhang, B.; Lacy, H. A.; Sparks, J. L.; Konkolewicz, D. Controlling Polymer Architecture to Design Dynamic Network Materials with Multiple Dynamic Linkers. *Mol. Syst. Des. Eng.* **2020**, *5* (7), 1267–1276.
- (5) Cuthbert, J.; Wanasinghe, S. V; Matyjaszewski, K.; Konkolewicz, D. Are RAFT and ATRP Universally Interchangeable Polymerization Methods in Network Formation? *Macromolecules* **2021**, *54* (18), 8331–8340.
- (6) YK, C. J. C.; Ercole, F. Living Free-Radical Polymerization by Reversible Addition—Fragmentation Chain Transfer: The RAFT Process. *Macromolecules* **1998**, *31*, 5559–5562.
- (7) Wang, R.; Luo, Y.; Li, B.-G.; Zhu, S. Modeling of Branching and Gelation in RAFT Copolymerization of Vinyl/Divinyl Systems. *Macromolecules* **2009**, *42* (1), 85–94.
- (8) Whitfield, R.; Parkatzidis, K.; Truong, N. P.; Junkers, T.; Anastasaki, A. Tailoring Polymer Dispersity by RAFT Polymerization: A Versatile Approach. *Chem* **2020**, *6* (6), 1340–1352.
- (9) Nothling, M. D.; Fu, Q.; Reyhani, A.; Allison-Logan, S.; Jung, K.; Zhu, J.; Kamigaito, M.; Boyer, C.; Qiao, G. G. Progress and Perspectives beyond Traditional RAFT Polymerization. *Adv. Sci.* **2020**, *7* (20), 2001656.
- (10) Pan, X.; Tasdelen, M. A.; Laun, J.; Junkers, T.; Yagci, Y.; Matyjaszewski, K. Photomediated Controlled Radical Polymerization. *Prog. Polym. Sci.* **2016**, *62*, 73–125.
- (11) Lehnen, A.-C.; Kurki, J. A. M.; Hartlieb, M. The Difference between Photo-Iniferter and Conventional RAFT Polymerization: High Livingness Enables the Straightforward

- Synthesis of Multiblock Copolymers. Polym. Chem. 2022, 13 (11), 1537–1546.
- (12) Foster, H.; Stenzel, M. H.; Chapman, R. PET-RAFT Enables Efficient and Automated Multiblock Star Synthesis. *Macromolecules* **2022**, *55* (14) 5938–5945.
- (13) Quinn, J. F.; Barner, L.; Barner-Kowollik, C.; Rizzardo, E.; Davis, T. P. Reversible Addition—Fragmentation Chain Transfer Polymerization Initiated with Ultraviolet Radiation. *Macromolecules* **2002**, *35* (20), 7620–7627.
- (14) Kwak, Y.; Matyjaszewski, K. Photoirradiated Atom Transfer Radical Polymerization with an Alkyl Dithiocarbamate at Ambient Temperature. *Macromolecules* 2010, 43 (12), 5180– 5183.
- (15) Zhou, H.; Johnson, J. A. Photo-controlled Growth of Telechelic Polymers and End-linked Polymer Gels. *Angew. Chemie* **2013**, *125* (8), 2291–2294.
- (16) Xu, J.; Shanmugam, S.; Corrigan, N. A.; Boyer, C. Catalyst-Free Visible Light-Induced RAFT Photopolymerization. In *Controlled Radical Polymerization: Mechanisms*; ACS Publications, 2015; pp 247–267.
- (17) Anastasaki, A.; Nikolaou, V.; Zhang, Q.; Burns, J.; Samanta, S. R.; Waldron, C.; Haddleton, A. J.; McHale, R.; Fox, D.; Percec, V. Copper (II)/Tertiary Amine Synergy in Photoinduced Living Radical Polymerization: Accelerated Synthesis of ω-Functional and α, ω-Heterofunctional Poly (Acrylates). *J. Am. Chem. Soc.* **2014**, *136* (3), 1141–1149.
- (18) Konkolewicz, D.; Schröder, K.; Buback, J.; Bernhard, S.; Matyjaszewski, K. Visible Light and Sunlight Photoinduced ATRP with Ppm of Cu Catalyst. *ACS Macro Lett.* **2012**, *I* (10), 1219–1223.
- (19) Yamago, S.; Ukai, Y.; Matsumoto, A.; Nakamura, Y. Organotellurium-Mediated Controlled/Living Radical Polymerization Initiated by Direct C- Te Bond Photolysis. *J. Am. Chem. Soc.* **2009**, *131* (6), 2100–2101.
- (20) Nakamura, Y.; Arima, T.; Yamago, S. Modular Synthesis of Mid-Chain-Functionalized Polymers by Photoinduced Diene-and Styrene-Assisted Radical Coupling Reaction of Polymer-End Radicals. *Macromolecules* **2014**, *47* (2), 582–588.
- (21) Xu, J.; Jung, K.; Atme, A.; Shanmugam, S.; Boyer, C. A Robust and Versatile Photoinduced Living Polymerization of Conjugated and Unconjugated Monomers and Its Oxygen Tolerance. *J. Am. Chem. Soc.* **2014**, *136* (14), 5508–5519.
- (22) Xu, J.; Shanmugam, S.; Fu, C.; Aguey-Zinsou, K.-F.; Boyer, C. Selective Photoactivation: From a Single Unit Monomer Insertion Reaction to Controlled Polymer Architectures. *J. Am. Chem. Soc.* **2016**, *138* (9), 3094–3106.
- (23) Shanmugam, S.; Xu, J.; Boyer, C. Photoinduced Electron Transfer–Reversible Addition–Fragmentation Chain Transfer (PET-RAFT) Polymerization of Vinyl Acetate and N-Vinylpyrrolidinone: Kinetic and Oxygen Tolerance Study. *Macromolecules* **2014**, *47* (15), 4930–4942.
- (24) Xu, J.; Jung, K.; Boyer, C. Oxygen Tolerance Study of Photoinduced Electron Transfer–Reversible Addition–Fragmentation Chain Transfer (PET-RAFT) Polymerization Mediated by Ru (Bpy) 3Cl2. *Macromolecules* **2014**, *47* (13), 4217–4229.
- (25) Allegrezza, M. L.; Konkolewicz, D. PET-RAFT Polymerization: Mechanistic Perspectives for Future Materials. *ACS Macro Lett.* **2021**, *10* (4), 433–446.
- (26) Kurek, P. N.; Kloster, A. J.; Weaver, K. A.; Manahan, R.; Allegrezza, M. L.; De Alwis Watuthanthrige, N.; Boyer, C.; Reeves, J. A.; Konkolewicz, D. How Do Reaction and Reactor Conditions Affect Photoinduced Electron/Energy Transfer Reversible Addition—Fragmentation Transfer Polymerization? *Ind. Eng. Chem. Res.* **2018**, *57* (12), 4203–4213.

- (27) Corrigan, N.; Xu, J.; Boyer, C.; Allonas, X. Exploration of the PET-RAFT Initiation Mechanism for Two Commonly Used Photocatalysts. *ChemPhotoChem* **2019**, *3* (11), 1193–1199.
- (28) Seal, P.; Xu, J.; De Luca, S.; Boyer, C.; Smith, S. C. Unraveling Photocatalytic Mechanism and Selectivity in PET-RAFT Polymerization. *Adv. theory simulations* **2019**, 2 (6), 1900038.
- (29) Wang, H.; Li, Q.; Dai, J.; Du, F.; Zheng, H.; Bai, R. Real-Time and in Situ Investigation of "Living"/Controlled Photopolymerization in the Presence of a Trithiocarbonate. *Macromolecules* **2013**, *46* (7), 2576–2582.

Table of Contents Entry Only

